

A Numerical-Analytical Hybrid Approach for the Identification of SDM Solar Cell Unknown Parameters

Rabeh Abbassi

College of Engineering, University of Hail, Saudi Arabia and University of Tunis, ENSIT, LaTICE Laboratory, Tunisia
r_abbassi@yahoo.fr

Attia Boudjemline

College of Engineering, University of Hail, Saudi Arabia
a_boudjemline@hotmail.com

Abdelkader Abbassi

Dept. of Electrical Engineering, University of Tunis, ENSIT, LISIER Laboratory, Tunisia
abd_abbassi@yahoo.com

Ahmed Torchani

College of Engineering, University of Hail, Saudi Arabia and University of Tunis, ENSIT, LISIER Laboratory, Tunisia
tochahm@yahoo.fr

Hatem Gasmi

College of Engineering, University of Hail, Saudi Arabia and University of Tunis El Manar, ENIT, Tunisia
gasmi_hatem@yahoo.fr

Tawfik Guesmi

College of Engineering, University of Hail, Saudi Arabia and University of Sfax, ENIS, Tunisia
tawfiq.guesmi@gmail.com

Abstract—Appropriate modeling and accurate parameter identification of solar cells are crucial in the optimization of photovoltaic (PV) systems. The single-diode model (SDM), consisting of an ideal current source, an ideal diode, a shunt resistor and a series resistor, is widely used to simulate the behavior of PV cells/panels. In this article, a hybrid approach for identification of solar cell SDM parameters is presented. This approach uses the inverse of the slope of the I-V curve under short-circuit and open-circuit conditions and combines numerical and analytical solutions. Indeed, knowing that numerical methods require appropriate initial values, the main idea of the proposed approach is to provide these solutions by analytical methods. The comparison of obtained results with experimental ones, based on manufacturer's datasheet, proves that the algorithm thus obtained requires less information from the manufacturer and improves significantly the parameter identification accuracy.

Keywords-solar energy; PV cell parameters; I-V and P-V characteristics; single-diode model

I. INTRODUCTION

Fossil fuels, i.e., oil, natural gas and coal, are the main sources of today's energy, whose demand is increasing in an alarming rate [1, 2]. In the process of extracting and converting these materials to energy, they generate air and water pollution, land degradation and, consequently, cause of harm to the health and well-being of humans and animals [3]. In addition, fossil fuels are non-renewable, as they exist in finite amounts. It is quite obvious that, at the present high rate of exploitation, they will eventually deplete rapidly, becoming too expensive to

extract [4]. So, we are faced with two enormous challenges: a decrease in the energy resources coupled with an increase in the damage to the environment [5, 6]. To mitigate these problems, efforts are being made worldwide by governments, national and international agencies, companies and research institutions to find other sources of energy that are renewable, sustainable, environment-friendly and not expensive [7-10]. In this respect, solar energy, in all its forms, has been identified as the most promising because it is plentiful, renewable, available in almost every country and harnessing it causes very little damage to the environment [10]. The most common method to exploit solar energy is via the photovoltaic (PV) effect, whereby the energy of the sunlight photons impinging on certain materials, is converted to electricity [11].

Photovoltaic panels are intended to work outdoors and, as such, are exposed to varying environmental conditions, e.g., temperature and amount of solar insolation. In order to predict the performance of PV systems, designers need to know the different electrical parameters of the PV cells/panel measured in all sorts of conditions. Unfortunately, PV manufacturers only provide some of the parameters at only one operating condition, referred to as standard test condition or STC [12]. To address this problem, designers and researchers resort to modeling the PV cells/panels in order to determine the vital intrinsic parameters. Although the main equations derived from these models are basically the same, numerous methods and techniques with varying degrees of complexity have been developed and applied with great success to estimate the parameters. Indeed, many review papers have been published to either summarize the salient features of these methods and/or to conduct a comparison between a few of them [13-20].

II. PV MODULE BASED ON SINGLE-DIODE MODEL

A. PV Cell Model

As mentioned above, it is of significant importance to know the performance of PV panels in different environmental conditions, e.g. solar irradiance and ambient temperature, before they are deployed in the field in order to maximize their output power [11, 21, 22]. In this respect, and due to the lack of information from datasheets, the intrinsic parameters that determine this performance need to be estimated. Since it is not practically possible to test all manufactured solar cells/panels under all types of conditions, engineers resort to simulations which result in saving materials, time and labor [23-25]. A PV cell is basically a diode, a p-n junction made of two dissimilar semiconducting materials, whose top surface is exposed to sunlight. The photon energy is subsequently converted to electrical energy. As a result, the most commonly-used equivalent electric circuit that describes the operation of a PV cell is the single-diode model as shown in Figure 1 (a) [26] and where the components are assumed ideal. In this model, I is the current delivered to the load and V is the voltage across the load. The current source represents the photoelectric current, I_{ph} , caused by the photons impinging on the solar cell. This current is assumed proportional to the solar irradiance and also depends on the cell's temperature [11]. The diode in parallel with the current source represents the recombination current in the quasi-neutral regions [27]. The current source serves to forward-bias the diode. The single-diode model has been shown to result in the calculation, to a high degree of accuracy, of the electrical parameters that are characteristic of the PV cells. It is a good compromise between precision and simplicity [29]. Furthermore, this model proved to be a very useful tool in optimizing the design of an entire PV system, including solar panels and control power electronics, and hence generating the maximum power possible. Note that, over the years, other equivalent electrical circuit models with different degrees of complexity and accuracy, such as double- and triple-diode ones, have been proposed depending on the desired outcomes; accuracy, time taken to simulate, etc. [11, 26, 27].

By applying Kirchhoff's current law to the equivalent circuit, which is a lossless model, the current at the terminals of the solar cell is expressed as:

$$I = I_{ph} - I_d = I_{ph} - I_o \left(e^{\frac{V}{\eta V_T}} - 1 \right) = I_{ph} - I_o \left(e^{\frac{qV}{\eta kT}} - 1 \right) \quad (1)$$

where,

- I_o : diode reverse bias saturation or dark current (A)
- η : diode ideality factor,
- V_T : thermal voltage (V)
- k : Boltzmann's constant ($=1.381 \times 10^{-23}$ J/K)
- q : charge of an electron ($=1.602 \times 10^{-19}$ Coulomb)
- T : cell's temperature in Kelvin (K).

Equation (1) shows the well-known Shockley diode equation. The diode reverse saturation current, I_o , originates

from minority carriers (e.g., electrons in the p-region) that recombine in the depletion region. This current limits the current in the reverse bias operation mode [28]. The ideality factor, η , also known as the quality factor or emission coefficient, depends on the fabrication process and semiconductor material. It is typically between 1 and 2, depending on the dominant recombination mechanism [14]. The thermal voltage, V_T , describes the voltage produced within the p-n junction due to temperature. At room temperature (300 K), $V_T \approx 26$ mV. A solar cell is characterized by its current-voltage (I-V) and power-voltage (P-V) curves. In order to generate accurate curves, one has to take into account the different losses associated with a cell/panel. Examples of the origins of these losses are intrinsic material defects, manufacturing flaws and the contacts with the loads. Consequently, a shunt resistor and a series resistor are added, as in Figure 1 (b), to give a more realistic electrical model.

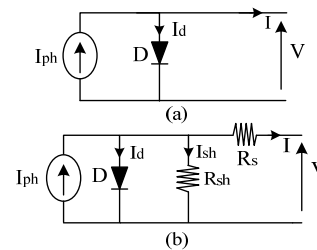


Fig. 1. Equivalent circuit of (a) ideal (b) practical SDM PV cell model.

The small series resistor R_s represents the conductivity of the materials, the thickness of the various layers and the ohmic contacts between metal and semiconductor [27]. The large shunt resistor R_{sh} represents the leakage current across the p-n junction when the diode is reverse-biased and usually originates from cell manufacturing defects [28]. Taking into account the two resistors, (1) becomes:

$$I = I_{ph} - I_d - I_{sh} \quad (2)$$

with

$$I_d = I_o \left[\exp\left(\frac{V_d}{\eta V_T}\right) - 1 \right] \quad (3)$$

$$V_d = V + IR_s \quad (4)$$

$$I_{sh} = \frac{V + IR_s}{R_{sh}} \quad (5)$$

By substituting (3), (4), and (5) in (2), we obtain:

$$I = I_{ph} - I_o \left[\exp\left(\frac{V + IR_s}{\eta V_T}\right) - 1 \right] - \frac{V + IR_s}{R_{sh}} \quad (6)$$

Equation (6) describes the current-voltage relationship of the PV cell and is the main equation used to represent the single-diode electrical model of Figure 1 (b) and also to plot the I-V and P-V curves. It is clear from (6) that, to calculate I as a function of V , the values of five parameters, namely, I_{ph} , I_o , R_s , R_{sh} and η need to be known. For most of the existing

panels, if not all of them, these parameters are not supplied by the manufacturers and hence need to be estimated.

B. Proposed Method Parameters Extraction

To determine the five independent parameters, five independent equations are required. It is customary to use data extracted from the PV panel datasheet and sometimes from experiments performed on the cell/panel. In particular, three values are used: the short circuit current I_{sc} , the open-circuit voltage V_{oc} and the maximum power generated P_{max} measured at the standard test conditions, STC, where the panel's ambient temperature is $T_c=25^\circ\text{C}$ (298 K), the irradiance is 1000W/m^2 and air mass AM1.5 [11]. The values resulting from the solution of the five equations are then used in subsequent simulations which force the modeled I-V and P-V curves to pass through these main three points. In what follows, the asterisk (*) denotes values measured at STC.

At open circuit: $I = 0, V = V_{oc}^*$ and (6) becomes:

$$I_{ph}^* = \left[\exp\left(\frac{V_{oc}^*}{\eta^* V_T}\right) - 1 \right] I_o^* + \frac{V_{oc}^*}{R_{sh}^*} \tag{7}$$

At short circuit: $V = 0, I = I_{sc}^*$ and (6) becomes:

$$I_{sc}^* - I_{ph}^* + \left[\exp\left(\frac{I_{sc}^* R_s^*}{\eta^* V_T}\right) - 1 \right] I_o^* + \frac{I_{sc}^* R_s^*}{R_{sh}^*} = 0 \tag{8}$$

Substituting (7) in (8) results in (9):

$$I_{sc}^* - \left[\exp\left(\frac{V_{oc}^*}{\eta^* V_T}\right) - \exp\left(\frac{I_{sc}^* R_s^*}{\eta^* V_T}\right) \right] I_o^* - \frac{V_{oc}^* - I_{sc}^* R_s^*}{R_{sh}^*} = 0 \tag{9}$$

At the maximum power $P_{max} : I = I_{mp}^*$ and $V = V_{mp}^*$: and (6) leads to (10):

$$I_{ph}^* - \left[\exp\left(\frac{V_{mp}^* + I_{mp}^* R_s^*}{\eta^* V_T}\right) - 1 \right] I_o^* - \frac{V_{mp}^* + I_{mp}^* R_s^*}{R_{sh}^*} - I_{mp}^* = 0 \tag{10}$$

By substituting (7) in (10) the latter becomes:

$$\left(1 + \frac{R_s^*}{R_{sh}^*}\right) I_{mp}^* - \left[\exp\left(\frac{V_{oc}^*}{\eta^* V_T}\right) - \exp\left(\frac{V_{mp}^* + I_{mp}^* R_s^*}{\eta^* V_T}\right) \right] I_o^* - \frac{V_{oc}^* - V_{mp}^*}{R_{sh}^*} = 0 \tag{11}$$

The power delivered to the load is $P = VI$ and its derivative with respect to the voltage V is:

$$\frac{dP}{dV} = I + V \frac{dI}{dV} \tag{12}$$

At the point of maximum power $P_{mp}^*, \frac{dP}{dV} \Big|_{P=P_{mp}^*} = 0$ and (12) becomes:

$$I_{mp}^* + V_{mp}^* \frac{dI}{dV} = 0 \tag{13}$$

The derivative of (6) gives:

$$\frac{dI}{dV} = -\frac{1}{\eta^* V_T} \left(1 + R_s \frac{dI}{dV}\right) \exp\left(\frac{V + IR_s}{\eta^* V_T}\right) I_o^* - \frac{1}{R_{sh}^*} \left(1 + R_s \frac{dI}{dV}\right) \tag{14}$$

At STC, and using (13) and (14), equation (15) is derived as follows:

$$\frac{I_{mp}^*}{V_{mp}^*} - \frac{1}{\eta^* V_T} \left(1 - R_s^* \frac{I_{mp}^*}{V_{mp}^*}\right) \left[\exp\left(\frac{V_{mp}^* + I_{mp}^* R_s^*}{\eta^* V_T}\right) \right] I_o^* - \frac{1}{R_{sh}^*} \left(1 - R_s^* \frac{I_{mp}^*}{V_{mp}^*}\right) = 0 \tag{15}$$

The result is a set of four non-linear equations, (7), (9), (11) and (15), with five unknown variables, $I_{ph}^*, I_o^*, R_s^*, R_{sh}^*$ and η^* . Consequently, a fifth equation is needed.

The slope of the I-V curve at short circuit, i.e., $I=I_{sc}^*$ and $V=0$, is approximately equal to the negative inverse of the shunt resistance R_{sho} [15, 29]. In other words,

$$\left. \frac{dI}{dV} \right|_{I=I_{sc}^* \text{ and } V=0} = -\frac{1}{R_{sho}} \tag{16}$$

With these values (14) will be rewritten as:

$$\frac{1}{R_{sho} - R_s^*} = \frac{1}{R_{sh}^*} + \frac{1}{\eta^* V_T} \exp\left(\frac{I_{sc}^* R_s^*}{\eta^* V_T}\right) I_o^* \tag{17}$$

In principle, R_{sho} can be extracted from the I-V curve, but since datasheets do not provide numerical values for the data used to plot this curve, researchers use graphical methods to achieve this by means of a digitizer. However, inaccurate values can result, which in turn will affect the other extracted parameters.

By assuming $(I_o^*/\eta^* V_T) \exp(I_{sc}^* R_s^*/\eta^* V_T) \square 1/R_{sh}^*$ and $R_{sho} \square R_s^*$, equation (17) will lead to the approximation $R_{sho} \approx R_{sh}^*$ [21]. Now, replacing R_{sho} by R_{sh}^* , in (17) will lead to:

$$\frac{1}{R_{sh}^* - R_s^*} = \frac{1}{R_{sh}^*} + \frac{1}{\eta^* V_T} \exp\left(\frac{I_{sc}^* R_s^*}{\eta^* V_T}\right) I_o^* \tag{18}$$

Finally, (7), (9), (11), (15) and (18) constitute a set of five non-linear equations with five unknown variables $I_{ph}^*, I_o^*, R_s^*, R_{sh}^*, \eta^*$.

Because these equations are inherently implicit and non-linear, finding analytical solutions is not a trivial task [24-30]. Approximations and simplifications are always used to arrive to some simple analytical solutions [25]. However, the set of transcendental equations is usually solved using numerical methods. These include curve-fitting, such as the Levenberg-Marquardt (LM) algorithm [29], and root-finding, such as the bisection and the Newton-Raphson methods [11, 21, 29]. To reach convergence, the numerical methods require good approximation of the starting values of the five parameters. To achieve this, analytical solutions are used. As a result, a variety of methods and techniques aiming at solving these non-linear equations have been devised, tested and published in the scientific literature over a few decades [12-22]. Once these parameters are determined, usually at STC, other equations are used to estimate the response of the PV cell/panel at other operating conditions, i.e., temperature and solar irradiance. Subsequently, (6) is used to generate the I-V curves for these operating conditions [11, 23, 26].

C. Approximate Analytical Solutions

From (9) the following expression for I_o^* is derived:

$$I_o^* = \frac{\left[\left((R_s^* + R_{sh}^*) I_{sc}^* - V_{oc}^* \right) / R_{sh}^* \right]}{\left[\exp(V_{oc}^* / \eta^* V_T) - \exp(I_{sc}^* R_s^* / \eta^* V_T) \right]} \tag{19}$$

The following acceptable assumptions and approximations are made. From experimental work, $R_{sh}^* \square R_s^*$, resulting in $1 + R_s^* / R_{sh}^* \approx 1$. In addition, $I_{sc}^* \square V_{oc}^* / R_{sh}^*$ and $\exp(V_{oc}^* / \eta^* V_T) \square \exp(I_{sc}^* R_s^* / \eta^* V_T)$ [31]. Equation (19) then becomes:

$$I_o^* = \exp(-V_{oc}^* / \eta^* V_T) I_{sc}^* \tag{20}$$

The shunt resistor R_{sh} has a high value, and is sometimes assumed infinite when modeling a PV cell. Furthermore, in short-circuit mode, the diode is reverse-biased and hence its current can be neglected. Consequently, the equality (21) is valid in all cases.

$$I_{ph}^* = I_{sc}^* \tag{21}$$

From the I-V and P-V curves, one can notice that $V_{oc}^* - V_{mp}^*$ is small and with R_{sh}^* being large, the following assumption: $(V_{oc}^* - V_{mp}^*) / R_{sh}^* \approx 0$ is valid. Hence, by substituting (20) and (21) in (11), we obtain (22):

$$I_{mp}^* = \left[1 - \exp\left((V_{mp}^* - V_{oc}^* + I_{mp}^* R_s^*) / \eta^* V_T \right) \right] I_{sc}^* \tag{22}$$

Since R_{sh}^* is high and $R_{sh}^* \square R_s^*$, the term $(1/R_{sh}^*) [1 - (R_{sh}^* I_{mp}^* / V_{mp}^*)]$ will be negligible and (15) becomes:

$$I_{mp}^* = (V_{mp}^* / \eta^* V_T) [1 - (R_{sh}^* I_{mp}^* / V_{mp}^*)] \times \left[\exp\left((V_{mp}^* - V_{oc}^* + I_{mp}^* R_s^*) / \eta^* V_T \right) \right] I_{sc}^* \tag{23}$$

Taking the previous assumptions into consideration, (18) is transformed as:

$$-R_s^* + \frac{(R_{sh}^*)^2 I_{sc}^*}{\eta^* V_T} \exp\left(\frac{I_{sc}^* R_s^* - V_{oc}^*}{\eta^* V_T} \right) = 0 \tag{24}$$

Equation (22) can be rewritten as:

$$\ln\left[(I_{sc}^* - I_{mp}^*) / I_{sc}^* \right] = (V_{mp}^* - V_{oc}^* + I_{mp}^* R_s^*) / \eta^* V_T \tag{25}$$

By eliminating the term $\exp\left[(V_{mp}^* - V_{oc}^* + I_{mp}^* R_s^*) / \eta^* V_T \right]$ from (22) and (23) and using (25), the following expressions for R_s^* and η^* are obtained [21]:

$$R_s^* = \frac{V_{mp}^*}{I_{mp}^*} - \frac{(2V_{mp}^* - V_{oc}^*) / (I_{sc}^* - I_{mp}^*)}{\left[\ln(1 - I_{mp}^* / I_{sc}^*) + I_{mp}^* / (I_{sc}^* - I_{mp}^*) \right]} \tag{26}$$

$$\eta^* = \frac{2V_{mp}^* - V_{oc}^*}{V_T \left[\ln(1 - I_{mp}^* / I_{sc}^*) + I_{mp}^* / (I_{sc}^* - I_{mp}^*) \right]} \tag{27}$$

Equation (24) leads to:

$$R_{sh}^* = \sqrt{\frac{R_s^*}{(I_{sc}^* / \eta^* V_T) \exp\left((I_{sc}^* R_s^* - V_{oc}^*) / \eta^* V_T \right)}} \tag{28}$$

Once R_s^* and η^* are computed using (26) and (27), their values will be used in (28) to calculate R_{sh}^* . The calculated values of R_s^* , η^* and R_{sh}^* , are in turn used to calculate I_o^* and I_{ph}^* from (19) and (7), respectively. Finally, and with the assumptions made, (7), (19), (26), (27) and (28) will constitute the approximated analytical solutions for the five parameters of the single-diode model for the PV cell/panel [32]. The estimated values of these parameters will be used as the starting values to solve numerically the implicit and nonlinear equations (7), (8), (11), (15) and (17) by the MATLAB ‘fsolve’ function based on L.M. algorithm.

D. Estimation of SDM Parameters at Operating Conditions

So far, the five SDM parameters were estimated at STC. However, in day-to-day applications, the conditions, especially the temperature and irradiance, are different from STC. Moreover, the cell/panel parameters depend strongly on these conditions. Therefore, it is crucial to evaluate the performance of the cell/panel at these real conditions. According to [12], the reverse saturation current I_o , the photocurrent I_{ph} and the shunt resistance R_{sh} are expressed as follows:

$$I_o = I_o^* \left(\frac{T}{T^*} \right)^3 \exp\left[\frac{1}{k} \left(\frac{E_g^*}{T^*} - \frac{E_g}{T} \right) \right] \tag{29}$$

$$I_{ph} = \frac{G}{G^*} [I_{ph}^* + k_i (T - T^*)] \tag{30}$$

$$R_{sh} = \frac{G^*}{G} R_{sh}^* \tag{31}$$

where: T , G , E_g and R_{sh} are the temperature, irradiance, material band gap energy and shunt resistance at the operating condition, respectively, whereas, T^* , G^* , E_g^* and R_{sh}^* are the corresponding parameters at STC. The parameter k_i is the temperature coefficient of the short-circuit current and k is Boltzmann’s constant.

III. RESULTS AND DISCUSSIONS

In this section, the extraction of the parameters of the proposed model is carried out. The results of the proposed optimization algorithm are compared with the experimental results. The comparison is implemented under different conditions of irradiation and temperature. The studied method was applied to the Suntech Power ‘STP250S-20/Wd’ monocrystalline silicon solar module and the multicrystalline Tallmax module ‘TSM-PD14’. The five parameters of the model were estimated in accordance with the main steps presented previously. Theoretical (or simulated) I-V and P-V curves derived from the developed approach were compared to experimental ones provided by the manufacturers, for different environmental conditions. The specifications of the ‘STP250S-20/Wd’ and ‘TSM-PD14’ panels are depicted in Table I. Figures 2 and 3 show the I-V and P-V characteristics of the ‘STP250S-20/Wd’ solar module at fixed module

temperature ($T=25^{\circ}\text{C}$) and under different irradiance levels (200, 400, 600, 800 and 1000W.m^{-2}). The curves were overlaid on top of those obtained using the proposed method to highlight any discrepancies. The model curves match well with the experimental data except for a negligible gap registered at high solar radiation. Similarly, Figures 4 and 5 depict the experimental I-V and P-V curves of the multicrystalline Tallmax solar module ‘TSM-PD14’. Again, one can see that the simulated model curves match well with the experimental ones. Figures 2, 3, 4 and 5 show the variation of I_{sc} (which is none other than I_{ph}) with the illumination. Moreover, the increase in solar radiation causes a slight rise in the open-circuit voltage in addition to an increase in the maximum power generated by the panel. These results prove that the calculated data are extremely close to the experimental ones.

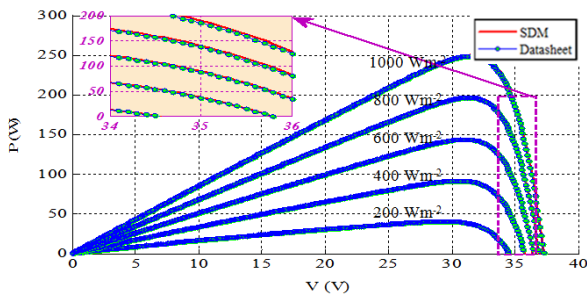


Fig. 2. Single-diode model and manufacturer datasheet P-V curves for STP250S-20/Wd at different irradiance levels (200, 400, 600, 800 and 1000W.m^{-2}) and fixed module temperature ($T=25^{\circ}\text{C}$).

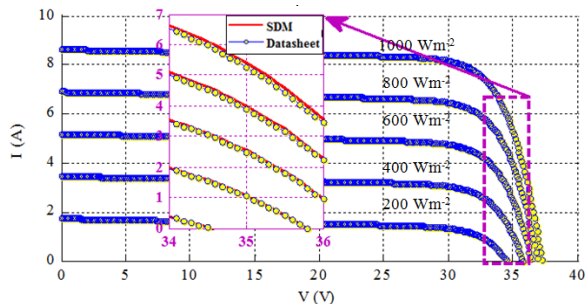


Fig. 3. Single-diode model and manufacturer datasheet I-V curves for STP250S-20/Wd at different irradiance levels (200, 400, 600, 800 and 1000W.m^{-2}) and fixed module temperature ($T=25^{\circ}\text{C}$).

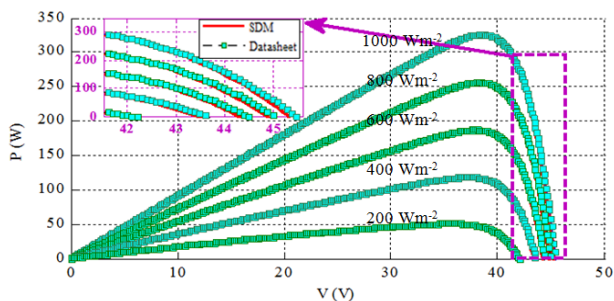


Fig. 4. Comparison of single-diode model and manufacturer datasheet P-V curve for TSM-PD14 at different irradiance levels (200, 400, 600, 800 and 1000W.m^{-2}) and fixed module temperature ($T=25^{\circ}\text{C}$).

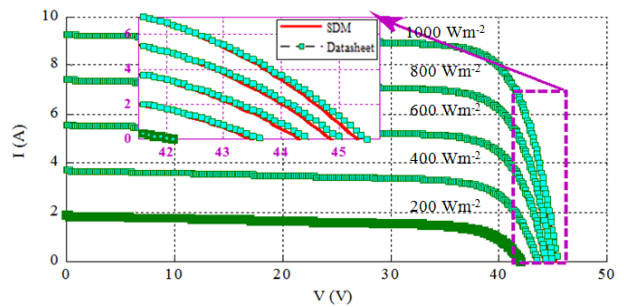


Fig. 5. Comparison of single-diode model and manufacturer datasheet I-V curve for TSM-PD14 at different irradiance levels (200, 400, 600, 800 and 1000W.m^{-2}) and fixed module temperature ($T=25^{\circ}\text{C}$).

TABLE I. DATASHEET OF SUNTECH-POWER ‘STP250S-20/Wd’ AND TALLMAX MODULE ‘TSM-PD14’ PV MODULES AT STANDARD TEST CONDITION (STC) AND NOMINAL OPERATING CELL TEMPERATURE (NOCT).

Datasheet parameters	STP250S-20/Wd		TSM-PD14	
	At STC	At NOCT	At STC	At NOCT
P_{mp}	250	183	325	242
V_{mp}	30.7	27.9	37.2	34.5
I_{mp}	8.15	6.55	8.76	7.02
V_{oc}	37.4	34.4	45.9	42.6
I_{sc}	8.63	6.96	9.25	7.47
k_i	0.05%/°C	-	0.05%/°C	-
k_v	0.34%/°C	-	0.32%/°C	-
N_s	60	-	72	-

After investigating the performance of the proposed approach under the effects of solar radiation, the effects of the temperature, which is a very important parameter, will also be evaluated. In order to predict a PV module I-V and P-V characteristics curves at different temperatures, for which data or I-V curves are not available, temperature coefficients (Temperature Coefficient of V_{oc} (k_v) and Temperature Coefficient of I_{sc} and (k_i)) were used. By using the Sandia National Laboratory database, the parameters $I_{sc}(T)$, $V_{oc}(T)$, $I_{mp}(T)$, and $V_{mp}(T)$, at different temperatures can be determined. Then, the obtained values enable the estimation of the those of $\eta(T)$, $I_o(T)$, and $I_{ph}(T)$. Subsequently, the I-V and P-V curves at 0°C , 25°C , 50°C , and 75°C were generated for the panels ‘STP250S-20/Wd’ and ‘TSM-PD14’ in Figures 6-9.

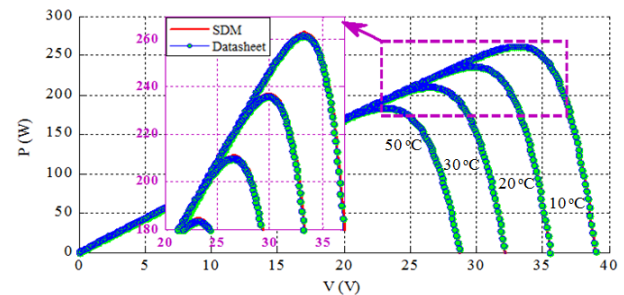


Fig. 6. Single-diode model and manufacturer datasheet P-V curves for STP250S-20/Wd at different module temperatures (10, 20, 30 and 50°C) and fixed irradiance level (1000W.m^{-2}).

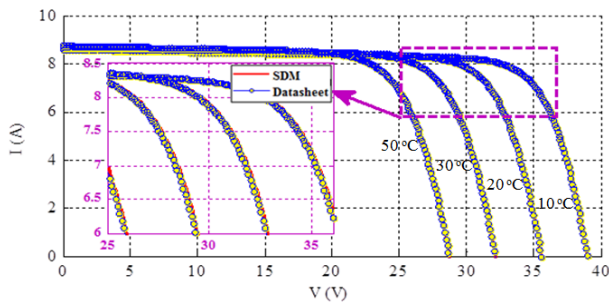


Fig. 7. Single-diode model and manufacturer datasheet I-V curves for STP250S-20/Wd at different module temperatures (10, 20, 30 and 50°C) and fixed irradiance level (1000W.m⁻²).

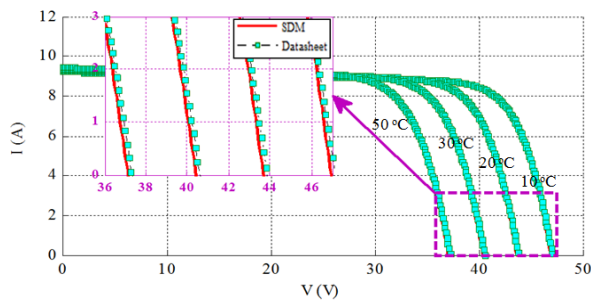


Fig. 8. Single-diode model and manufacturer datasheet I-V curves for TSM-PD14 at different module temperatures (10, 20, 30 and 50°C) and fixed irradiance level (1000W.m⁻²).

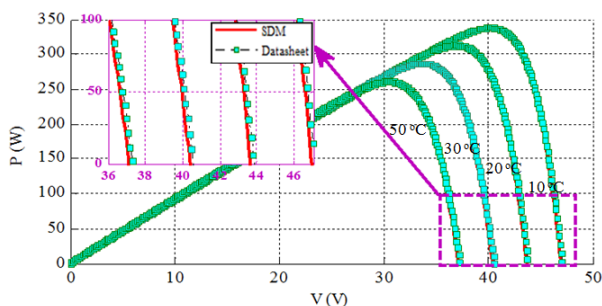


Fig. 9. Single-diode model and manufacturer datasheet P-V curves for TSM-PD14 at different module temperatures (10, 20, 30 and 50°C) and fixed irradiance level (1000W.m⁻²).

While increasing the temperature lead to a negligible increase in the photocurrent I_{ph} due to better light absorption, a noticeable decrease in the open-circuit voltage is observed. This is accompanied by a large reduction in the maximum power P_{max} which translates into a decrease in the available power. The superposition of the I-V and P-V curves obtained using the estimated parameters (of the single-diode model adopted in the work presented here) on top of those generated using the experimental data show very good agreement albeit negligible differences.

IV. CONCLUSIONS

In this paper, a hybrid numerical-analytical approach was developed and programmed in MATLAB environment. Its capability to estimate the unknown electrical parameters of PV

modules using single-diode model (SDM) was validated by the experimental I-V and P-V data extracted from the manufacturer's datasheet. Two PV modules, namely, 'STP250S-20/Wd' and 'TSM-PD14', made with different manufacturing techniques were utilized for validation. It can be concluded that the extracted characteristics nearly coincide with the experimental ones. Consequently, the obtained good fitting indicates the feasibility and high precision of the proposed method.

REFERENCES

- [1] F. T. Hamzehkolaei, N. Amjadi, "A techno-economic assessment for replacement of conventional fossil fuel based technologies in animal farms with biogas fueled CHP units", *Renewable Energy*, Vol. 118, pp. 602-614, 2018
- [2] S. Saad, L. Zellouma, "Fuzzy logic controller for three-level shunt active filter compensating harmonics and reactive power", *Electric Power Systems Research*, Vol. 79, No. 10, pp. 1337-1341, 2009
- [3] A. Nikolaev, P. Konidari, "Development and assessment of renewable energy policy scenarios by 2030 for Bulgaria", *Renewable Energy*, Vol. 111, pp. 792-802, 2017
- [4] M. A. Destek, A. Aslan, "Renewable and non-renewable energy consumption and economic growth in emerging economies: Evidence from bootstrap panel causality", *Renewable Energy*, Vol. 111, pp. 757-763, 2017
- [5] R. Abbassi, S. Marrouchi, M. Ben Hessine, S. Chebbi, H. Jouini, "Voltage Control Strategy of an Electrical Network by the Integration of the UPFC Compensator", *International Review On Modelling and Simulation*, Vol. 5, No. 1, pp. 380-384, 2012
- [6] M. Bhattacharya, S. A. Churchill, S. R. Paramati, "The dynamic impact of renewable energy and institutions on economic output and CO2 emissions across regions", *Renewable Energy*, Vol. 111, pp. 157-167, 2017
- [7] R. Abbassi, S. Saidi, M. Hammami, S. Chebbi, "Analysis of renewable energy power systems: Reliability and flexibility during unbalanced network fault", in: *Handbook of Research on Advanced Intelligent Control Engineering and Automation*, pp. 651-686, IGI Global, 2015
- [8] K. Hori, T. Matsui, T. Hasuike, K. Fukui, T. Machimura, "Development and application of the renewable energy regional optimization utility tool for environmental sustainability: REROUTES", *Renewable Energy*, Vol. 93, pp. 548-561, 2016
- [9] R. Abbassi, S. Chebbi, "Energy Management Strategy for a Grid-Connected Wind-Solar Hybrid System with Battery Storage: Policy for Optimizing Conventional Energy Generation", *International Review of Electrical Engineering*, Vol 7, pp. 3979-3990, 2012
- [10] A. Abbassi, M. A. Dami, M. Jemli, "A statistical approach for hybrid energy storage system sizing based on capacity distributions in an autonomous PV/Wind power generation system", *Renewable Energy*, Vol. 103, pp. 81-93, 2017
- [11] A. Abbassi, R. Gammoudi, M. A. Dami, O. Hasnaoui, M. Jemli, "An improved single-diode model parameters extraction at different operating conditions with a view to modeling a photovoltaic generator: A comparative study", *Solar Energy*, Vol. 155, pp. 478-489, 2017
- [12] W. De Soto, S. A. Klein, W. A. Beckman, "Improvement and validation of a model for photovoltaic array performance", *Solar Energy*, Vol. 80, No. 1, pp. 78-88, 2006
- [13] D. T. Cotfas, P. A. Cotfas, S. Kaplanis, "Methods to determine the dc parameters of solar cells: A critical review", *Renewable and Sustainable Energy Reviews*, Vol. 28, pp. 588-596, 2013
- [14] G. Ciulla, V. Lo Brano, V. Di Dio, G. Cipriani, "A comparison of different one-diode models for the representation of I-V characteristic of a PV cell", *Renewable and Sustainable Energy Reviews*, Vol. 32, pp. 684-696, 2014
- [15] D. Jena, V. V. Ramana, "Modeling of photovoltaic system for uniform and non-uniform irradiance - A critical review", *Renewable and Sustainable Energy Reviews*, Vol. 52, pp. 400-417, 2015

- [16] A. M. Humada, M. Hojabri, S. Mekhilef, H. M. Hamada, "Solar cell parameters extraction based on single and double-diode models: A review", *Renewable and Sustainable Energy Reviews*, Vol. 28, pp. 494-509, 2016
- [17] M. U. Siddiqui, A. F. M. Arif, A. M. Bilton, S. Dubowsky, M. Elshafei, "An improved electric circuit model for photovoltaic modules based on sensitivity analysis", *Solar Energy*, Vol. 90, pp. 29-42, 2013
- [18] M. B. H. Rhouma, A. Gastli, L. B. Brahim, F. Touati, M. Benammar, "A simple method for extracting the parameters of the PV cell single-diode model", *Renewable Energy*, Vol. 113, pp. 885-894, 2017
- [19] M. Bashahu, A. Habyarimana, "Review and test of methods for determination of the solar cell series resistance", *Renewable Energy*, Vol. 6, No 2, 129-138, 1995
- [20] W. Gong, Z. Cai, "Parameter extraction of solar cell models using repaired adaptive differential evolution", *Solar Energy*, Vol. 94, pp. 209-220, 2013
- [21] M. Hejri, H. Mokhtari, M. R. Azizian, L. Söder, "An analytical-numerical approach for parameter determination of a five-parameter single-diode of photovoltaic cells and modules", *International Journal of Sustainable Energy*, Vol. 35, No. 4, pp. 396-410, 2016
- [22] P. A. Kumari, P. Geethanjali, "Parameter estimation for photovoltaic system under normal and partial shading conditions: A survey", *Renewable and Sustainable Energy Reviews*, Vol. 84, pp. 1-11, 2018
- [23] N. Barth, R. Jovanovic, S. Ahzi, M. A. Khaleel, "PV panel single and double diode models: Optimization of the parameters and temperature dependence", *Solar Energy Materials and Solar Cells*, Vol. 148, pp. 87-98, 2016
- [24] S. Bana, R.P. Saini, "Identification of unknown parameters of a single diode photovoltaic model using particle swarm optimization with binary constraints", *Renewable Energy*, Vol. 101, pp.1299-1310, 2017
- [25] F.J. Toledo, J. M. Blanes, "Analytical and quasi-explicit four arbitrary point method for extraction of solar cell single-diode model parameters", *Renewable Energy*, Vol. 92, pp. 346-356, 2016
- [26] K. Ishaque, Z. Salam, S. Mekhilef, A. Shamsudin, "Parameter extraction of solar photovoltaic modules using penalty-based differential evolution", *Applied Energy*, Vol. 99, pp. 297-308, 2012
- [27] A. Luque, S. Hegedus, *Handbook of Photovoltaic Science and Engineering*, John Wiley & Sons, Ltd, 2005
- [28] H. Wirth, *Photovoltaic Modules - Technology and Reliability*, Walter de Gruyter GmbH & Co KG, 2016
- [29] G. Petrone, C. A. Ramos-Paja, G. Spagnuolo, *Photovoltaic Sources Modeling*, Wiley & Sons, 2017
- [30] M. Chegaar, Z. Ouennoughi, F. Guechi, "Extracting dc parameters of solar cells under illumination", *Vacuum*, Vol. 75, No 4, pp. 367-372, 2004
- [31] J. C. H. Phang, D. S. H. Chan, J. R. Phillips, "Accurate analytical method for the extraction of solar cell model parameters", *Electronics Letters*, Vol. 20, No. 10, pp. 406-408, 1984
- [32] M. Kumar, A. Kumar, "An efficient parameters extraction technique of photovoltaic models for performance assessment", *Solar Energy*, Vol. 158, pp. 192-206, 2017